J Solid State Electrochem (2008) 12:1279–1284
DOI 10.1007/s10008-008-0510-x

ORIGINAL PAPER

In situ optical spectroelectrochemistry of single-walled carbon nanotube thin films

Markéta Zukalová · Ján Tarábek · Martin Kalbáč · Ladislav Kavan · Lothar Dunsch

Received: 25 November 2007 / Revised: 22 December 2007 / Accepted: 6 January 2008 / Published online: 31 January 2008

Abstract A detailed study is presented on the optical absorption of thin films of single-walled carbon nanotubes (SWNT) under electrochemical conditions. The procedure for the preparation of free-standing semitransparent films of SWNT is used for the fabrication of a working electrode for transmission optical spectroelectrochemistry. The analysis of the potential dependent spectroscopic response of the SWNT film benefits from the widest possible electrochemical window, in which the charging of SWNT can safely be investigated. This electrochemical window is not limited by parasitic electrochemistry and/or galvanic breakdown reactions occurring at supporting electrode materials such as indium–tin oxide conducting glass or semitransparent Pt film, which were employed in earlier studies. Electrochemical doping of SWNT is observable at the optical absorptions, which are assigned to allowed electronic transitions between van Hove singularities in the density of states of SWNT. Furthermore, the spectral response of counterions, balancing the charging of the nanotube skeleton, is traceable at certain conditions. The latter effect is monitored here through the overtones of C–H stretching vibrations from tetrabutylammonium cations.

M. Zukalová · J. Tarábek · M. Kalbáč · L. Kavan (✉)
J. Heyrovsky Institute of Physical Chemistry, v.v.i.,
Academy of Sciences of the Czech Republic,
Dolejskova 3,
182 23 Prague 8, Czech Republic
e-mail: ladislav.kavan@jh-inst.cas.cz

M. Zukalová · J. Tarábek · M. Kalbáč · L. Dunsch (✉)
Group of Electrochemistry and Conducting Polymers,
Leibniz Institute of Solid State and Materials Research,
Helmholtzstr. 20,
01069 Dresden, Germany
e-mail: l.dunsch@ifw-dresden.de

Keywords UV-Vis spectroelectrochemistry · Cyclic voltammetry · Single-walled carbon nanotubes · Thin films · Doping

Introduction

The optical spectra of single-walled carbon nanotubes (SWNT) are understood in terms of allowed electronic transitions between van Hove singularities (vHS) in the density of states. Within the approximation of a tight binding model, the energy separations between the *i*-th singularities, ΔE_{ii}, scale with the tube diameter, *d*:

$$\Delta E_{ii} = \frac{2i\gamma_0 a_{C-C}}{d} + \delta E \quad (1)$$

where γ_0 is the nearest neighbor overlap integral ($\gamma_0 \cong$ 2.5 eV), a_{C-C} is the distance of C-atoms in graphene (a_{C-C} $\cong$0.142 nm), and δE ($\cong$0.2 eV) is a correction for intertube interaction in a bundle. The semiconducting tubes exhibit well resolved optical absorption bands for the first two pairs of singularities, ΔE_{11}^{S}, ΔE_{22}^{S}, and metallic tubes for the first-pair transition, ΔE_{11}^{M}. The tube diameter, *d*, correlates with the chiral indices, (*n*, *m*), which define the geometry of graphene rolling:

$$d = \frac{a_{C-C}\sqrt{3}}{\pi}\sqrt{n^2 + m^2 + nm} \quad (2)$$

Redox doping of single-walled carbon nanotubes influences these optical transitions as long as the population of VHS is tuned by charge transfer. This strategy was started in 1997 by Rao et al. [1], who used electron donor/acceptor molecules as doping agents as well as Raman spectroscopy for monitoring of the doping effect. Two years later, Eklund et al. [2] combined, for the first time, Raman spectroscopy with electrochemical doping.

Although these two classical works [1, 2] were concentrated solely on the doping-induced changes of Raman frequencies, the most pronounced effect is, obviously, the Raman intensity attenuation. It sets in as a result of erasing of the resonance enhancement via optical transitions between vHS (Eq. 1) [3, 4]. This effect also points at the principal limitation of Raman scattering: Because of the strongly selective resonance enhancement, a single Raman experiment is principally unable to address all the (*n*, *m*) tubes, which are present in a conventional sample (Eqs. 1 and 2). On the other hand, visible–near infrared (Vis–NIR) spectroscopy allows a direct addressing of optical transitions between VHS in all tubes in one experiment.

Electrochemistry, as a method of choice for the SWNT charging, benefits from precise control of the doping level and a broad selection of compensating counterions of the electrolytes. This is a clear advantage over the application of chemical redox reactants. In the latter case, the doping level is poorly controllable, and there are only few redox molecules, which can act as net electron/hole donors without parasitic chemical modification of the SWNT surface. Therefore, the in situ optical and Raman spectroelectrochemistry techniques provide the detailed information on SWNT and other carbon nanostructures [5].

The Vis–NIR spectra of redox doped SWNT were first studied by Kazaoui et al. [6] and Petit et al. [7] in 1999. Both these pioneering works employed the chemical redox doping, either with gaseous Br_2 or I_2 as electron acceptors (p-doping) or K, Cs, and organic radical anions as electron donors (n-doping). Besides the attenuation of the optical bands ΔE_{11}^{S}, ΔE_{22}^{S}, and ΔE_{11}^{M}, there was also a secondary effect, called doping-induced absorption [6], which was tentatively assigned to transitions within partly filled valence (p-doping) or conduction (n-doping) bands [6, 8], modification of the π-plasmon background [9] or to the creation of new free-charge-carrier plasmons [10].

In 2000, in situ Vis–NIR spectroelectrochemistry of SWNT was pioneered by Kavan et al. [3]. The bleaching of optical transitions ΔE_{11}^{S}, ΔE_{22}^{S}, and ΔE_{11}^{M} was traceable upon adjusting the electrochemical potential of a layer of SWNT on indium–tin oxide (ITO) [3, 4, 11] or semitransparent Pt film [12, 13] in aqueous [3] or acetonitrile [4, 12, 13] electrolyte solutions or in ionic liquids [11], viz. tetrafluoroborate or hexafluorophosphate salts of 1-butyl-3-methylimidazolium. The charging-induced attenuation of optical bands was reversible in the time domain of seconds [4, 11]. The analogy of chemical and electrochemical doping extended even to the appearance of new doping-induced transitions for heavy electrochemical doping [4, 11].

This paper refers to our previous works on the optical spectroelectrochemistry of SWNT [3, 4, 11] and presents a new level of the spectroelectrochemical characterization of SWNT. In particular, we have employed an advanced technique for the SWNT thin film fabrication, which allowed us to avoid the use of ITO conducting glass for the fabrication of the working electrode for spectroelectrochemistry. This is beneficial especially for deep n-doping, because ITO is unstable at highly cathodic potentials. To the best of our knowledge, the strategy of using a sole semitransparent film of SWNT is demonstrated here for the first time. Second, we have chosen a different electrolyte solution than in the earlier works [3, 4, 11] to demonstrate the differentiation of a double-layer charging and Faradaic reactions on the Vis–NIR spectra of SWNT. This reasoning stems from our recent suggestion that the quenching of vHS can be formally regarded as a Faradaic current from or to the singularities [5]. Therefore, the current response in cyclic voltammetry is not solely due to a double layer charging but also due to Faradaic processes at many redox potentials that are distributed over a larger range of (*n, m*) tubes. Hence, no distinct voltammetric peak is detected.

Experimental section

Materials

Single-walled carbon nanotubes were from Tubes@Rice (sample No. P06049-6). They are laser-ablation grown tubes with a diameter distribution between 1.1 to 1.4 nm [4]. Three hundred milligrams of SWNT was dispersed in toluene/acetone mixture (1:1, *v*/*v*) by sonication (ultrasonic bath, Transsonic Elma T 470/H, P-Lab, Czech Republic) for 20 min. The suspension was stored for about 2 h and subsequently vacuum filtered through a polytetrafluoroethylene membrane (diameter=25 mm, pore size=0.2 μm, Whatman, England) until dryness (approximately 20 min). The thus obtained buckypaper was dried at 200 °C/0.1 Pa for 8 h. This material served as a starting SWNT sample for the preparation of transparent films.

Preparation of electrodes

Transparent SWNT films were prepared as sketched in Fig. 1. A portion of buckypaper (see above) was dispersed in 1% aqueous (*w*/*w*) Triton X-100 (polyethylene glycol *tert*-octylphenyl ether, for molecular biology, Fluka, Germany) by sonication for 30 min. Suspension of SWNT was prepared with two different mass concentrations: $\rho_1 \approx 3 \times 10^{-6}$ gml^{-1} and $\rho_2 \approx 7 \times 10^{-6}$ g ml^{-1}. In the next, ≈25 ml of suspension of a given concentration was transferred into a 50-ml centrifuge plastic vessel and successively centrifuged (MR 23i centrifuge, Jouan, France) as shown in Table 1. The finally obtained supernatant (≈20 ml, carefully decanted with

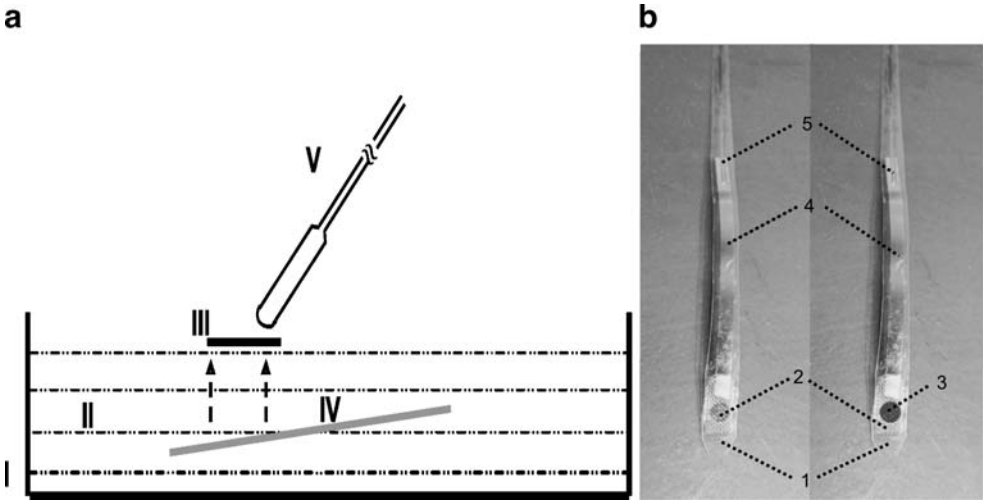

Fig. 1 **a** Scheme of the fabrication of the SWNT thin film working electrode: *I* Petri dish, *II* acetone, *III* thin SWNT film (MCE membrane already dissolved), *IV* laminated electrode, *V* spatula. **b** Laminated Pt-μ-mesh electrode without and with the SWNT film, respectively: *1* lamination foil, *2* Pt-μ-mesh, *3* SWNT film, *4* gold foil, *5* Cu-wire

Pasteur pipette) was filtered through the surfactant-free mixed cellulose ester (MCE) membrane filter disc (cellulose nitrate + cellulose acetate, diameter of 25 mm, pore size of 0.22 μm, Millipore, USA). The residual surfactant in the SWNT film was washed away with water (300–500 ml) in the vacuum filtration apparatus while the pump was still running. Vacuum suction was on until the film was completely dry (30–40 min), and the MCE-filter disc with the adhering SWNT film (diameter=15 mm) was kept back. Deionized water with the conductivity of $\leq 10^{-6}$ Scm^{-1}, toluene (99.8%, http://medical-dictionary.thefreedictionary.com/chromatography high-performance liquid chromatography grade), and acetone (≥99.5%, p.a.) were used as solvents.

The SWNT film covered membrane filter was immersed in a Petri dish filled with acetone. The MCE membrane dissolved leaving the nanotube film floating on the acetone surface. Finally, the SWNT film was carefully picked up with a platinum or gold μ-mesh and transferred to the acetone bath for ≈30 min. Washing in acetone bath was repeated several times to ensure the complete removal of the MCE membrane. Alternatively, the semitransparent SWNT film was deposited on an ordinary microscope cover glass instead of Pt or Au μ-mesh. The transport of the film onto the glass surface was done in a large diameter (≈180 mm) Petri dish. The microscope cover glass was immersed into the acetone bath directly under the floating SWNT film, which was carefully picked up. After drying, the SWNT film on the glass support was contacted with the gold ribbon connected with the gold wire. The electrode was finally covered with polyester-based laminating foil (DocuSeal, 100-μm thickness, General Binding, USA) leaving just 0.03 cm^2 of active electrode surface uncovered, to avoid short circuiting when placed in the glass 1-mm thick cuvette, representing the spectroelectrochemical cell.

Vis–NIR spectroelectrochemical measurements

Vis–NIR spectroscopy was measured with a double-beam Shimadzu MPC 3100 spectrometer. The reference blank was a pure electrolyte solution. Electrochemical experiments were carried out using PG 300 (HEKA) or PAR 263A (EG&G) potentiostats with Pt auxiliary and Ag-wire pseudo-reference electrodes; the electrolyte solution was a 0.1 M tetrabutylammonium tetrafluoroborate $[(C_4H_9)_4NBF_4]$ in acetonitrile (both from Aldrich; the latter dried by a 4-Å molecular sieve). The cell was assembled in a glove box (M. Braun); the box atmosphere was N_2 containing <1 ppm of both O_2 and H_2O.

Table 1 Overview of the prepared thin films of SWNT (see Experimental section for details)

Sample	Parent material	First centrifugation	Second centrifugation	Third centrifugation
1	SWNT suspension, $\rho=3.10^{-6}$g/ml			
2A	SWNT suspension, $\rho=3.10^{-6}$g/ml	10 min at 800 g	40 min at 8,000 g	
2B	SWNT suspension, $\rho=7.10^{-6}$g/ml	10 min at 800 g	40 min at 8,000 g	
3A	SWNT suspension, $\rho=3.10^{-6}$g/ml	10 min at 1,600 g	40 min at 16,000 g	
3B	SWNT suspension, $\rho=7.10^{-6}$g/ml	10 min at 1,600 g	40 min at 16,000 g	
4	SWNT suspension, $\rho=7.10^{-6}$g/ml	10 min at 1,600 g	40 min at 16,000 g	60 min at 20,000 g

Results and discussion

Our method of producing semitransparent films from pure SWNT stems from the pioneering work of Wu et al. [14]. Obviously, this film can be, eventually, competitive to ITO in terms of electrical conductivity and optical transparency in the Vis–NIR region [14]. With regard to the known sensitivity of ITO toward reductive breakdown, it is desirable to avoid this material in spectroelectrochemistry, especially if n-doping is investigated. The problem of the limited electrochemical window is addressable either by using inert (Au, Pt) microgrid for electrical contact to SWNT or by fabricating a pure SWNT film acting as the working electrode without any other supporting electrode material. The latter method is the most elegant one, but surprisingly, and to the best of our knowledge, it is presented here for the first time.

Figure 2 shows the spectra of dry SWNT films on glass. The corresponding transitions ΔE_{11}^{S}, ΔE_{22}^{S}, and ΔE_{11}^{M} are distinguishable at approximately 0.7, 1.2, and 1.8 eV, respectively. This confirms that our sample is a polydisperse mixture of SWNT having diameters between approximately 1.1 and 1.4 nm (Eqs. 1 and 2). It is obvious that the absorbance is roughly doubled for films 2B and 3B as compared to films 2A and 3A. The reason is that the films 2B and 3B were prepared from the starting suspension with higher ρ than 2A and 3A. Moreover, the individual bands of the films 2A, 2B, 3A, 3B, and 4 are more pronounced than the bands of the film 1. This is obviously due to the fact that the supernatant after centrifugation is purified from the carbonaceous impurities in the starting material and from defect tubes, which can cause broadening of the characteristic Vis–NIR bands.

There are also slight shifts of the bands corresponding to the ΔE_{11}^{S}, ΔE_{22}^{S} transitions. This is a consequence of the fact that centrifugation causes small changes in the composition of the nanotubes mixture. Nevertheless, centrifugation at the used conditions (see Experimental section) does not lead to any significant enrichment of tubes with defined diameters and/or chiralities (for efficient sorting of the mixture, one would ideally require ultracentrifugation in a density-gradient medium [15]).

The glass-supported thin film of SWNT has a sufficient electrical conductivity and therefore favorable electrochemical properties to be used as a working electrode in potentiostatic regime. This is documented in Fig. 3, which shows a cyclic voltammogram of our working electrode from the film 2B (see Table 1) measured directly in the actual spectroelectrochemical cell (cf. Fig. 1) after adding approximately 10^{-4} M ferrocene to the electrolyte solution. The other prepared films exhibited similar performance (data not shown). The voltammogram is slightly perturbed by iR drop, but, in general, comparable to that measured in a classical system with SWNT deposited on a metallic substrate (compare Fig. 1 in [4], which shows a plot of cyclic voltammogram of a similar SWNT sample, but deposited directly on a Pt current collector and without ferrocene addition).

We should note that the cell geometry (cf. Fig. 1) is dictated by the requirements of the Vis–NIR spectroscopic measurement; hence, it is not in the optimum configuration from the point of view of electrochemical experiment. Nevertheless, even this nonideal geometry still provides

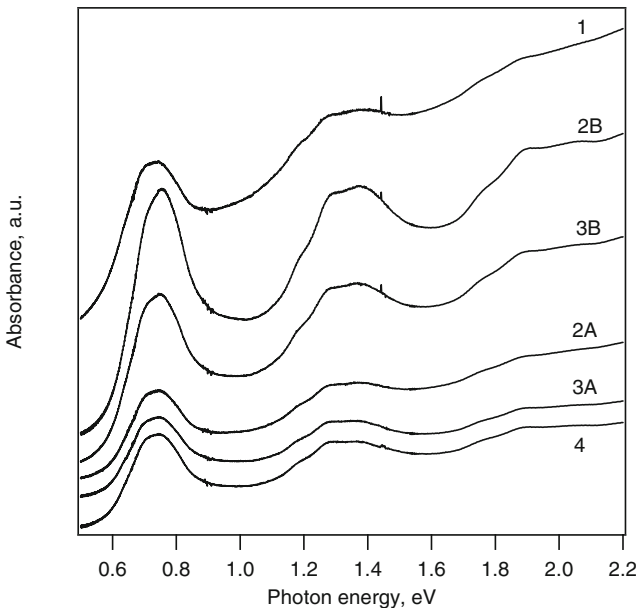

Fig. 2 Vis–NIR spectra of dry SWNT films on glass. The spectra are offset for clarity, but the intensity scale is identical for all spectra. The *curves* are labeled by the codes of the particular SWCNT films, see Table 1 and Experimental section

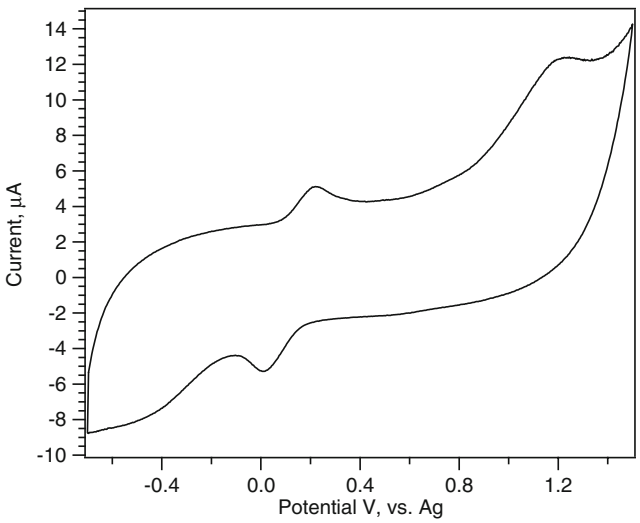

Fig. 3 Cyclic voltammogram of a thin SWNT film (2B, see Table 1) deposited on glass. The voltammogram was measured after the electrode passed the Vis–NIR spectroelectrochemical test. The electrolyte was 0.1 M $(C_4H_9)_4NBF_4$ + acetonitrile with an approximately 10^{-4} M ferrocene addition. Scan rate=10 mV/s

acceptable electrochemical behavior in cyclic voltammetry. This is documented on a model redox couple, viz. ferrocene, which was deliberately added to the electrolyte solution. The peak-to-peak splitting is approximately 200 mV (Fig. 3), which is larger than the theoretically expected value of a reversible redox system. The origin of an irreversible anodic peak at about 1.2 V is unclear. Peaks typically occur at voltammograms of functionalized SWNT and might be ascribed to Faradaic contribution of surface oxides [4]. Nevertheless, for a spectroelectrochemical measurement at a constant potential in steady state conditions (*vide infra*), the potential control is reliable for this kind of cell and working electrode configuration.

Before addition of ferrocene, the cyclic voltammogram of our nanotube film is featureless (data not shown) and, essentially, very similar to the voltammogram measured on a Pt-supported SWNT layer [4]. From the voltammetric current (I) near the potentials of the "double-layer regime," we can estimate the electrochemical capacitance:

$$C = I/vm \tag{3}$$

to be approximately 40 F/g [4] (v is the scan rate, and m is the mass of SWNT film).

Figure 4 shows the spectroelectrochemical plot of our glass-supported SWNT film. We trace the expected attenuation of absorption bands starting from ΔE_{11}^{S} and progressing toward ΔE_{22}^{S} and ΔE_{11}^{M}. Furthermore, we can find the doping-induced transitions. Of particular interest is the possibility of carrying out measurements down to −1.8 V vs. Ag-pseudoreference electrode. These potentials were not accessible in earlier studies of ITO-supported SWNT films [3–5] due to instability of ITO against cathodic decomposition. In addition, the semitransparent Pt electrode [12, 13] does not seem to be optimal for measurements at deeply cathodic potentials, because of the electrocatalytic activity of platinum, which promotes cathodic breakdown reactions in the electrolyte solution.

Another novel feature, which has not been observed so far in earlier works on optical spectroelectrochemistry of SWNT [3–5, 11], are two sharp bands at 0.72 and 0.74 eV. They occur in the region, where the overtones of the C–H stretching vibration are expected (at approximately 5,900 cm^{-1}; cf. Fig. 4). We suggest their assignment to the tetrabutylammonium cation, NBu_4^+, as the fundamental frequencies of C–H stretch in NBu_4^+ make a doublet IR feature at 2,960 and 2,946 cm^{-1} (data not shown). Strictly speaking, the assignment of the doublet in Fig. 4 to NBu_4^+ is not unique, because the acetonitrile solvent has strong bands in this region, too. As, however, the spectra are subtractive normalized against a pure electrolyte solution (see Experimental section), the changes in optical densities reflect the relative changes in concentration of a C–H containing species as a result of different electrochemical

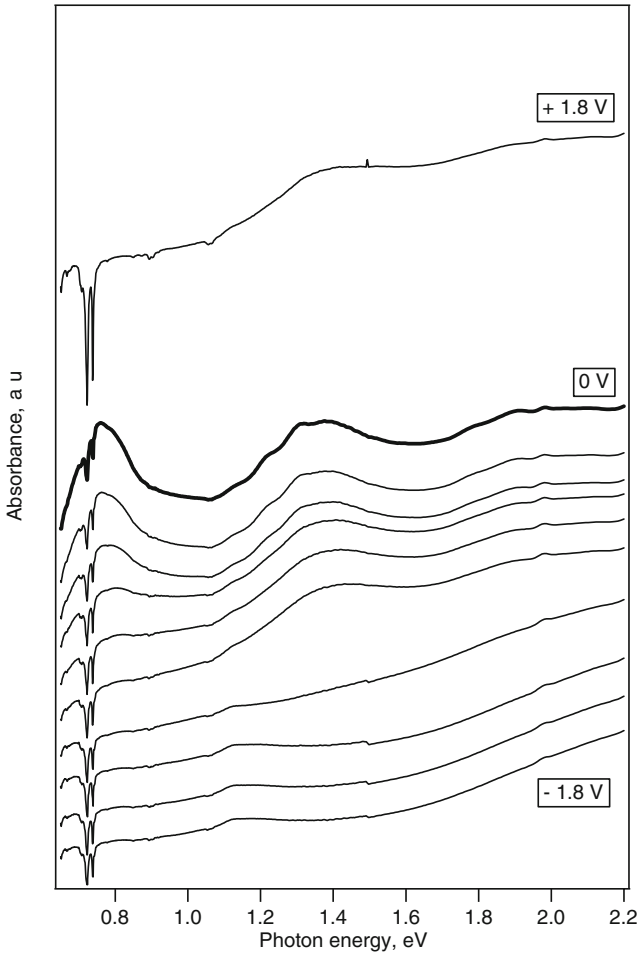

Fig. 4 Potential-dependent Vis–NIR spectra of SWNT on glass in 0.1 M $(C_4H_9)_4NBF_4$ + acetonitrile. The spectrum in nearly undoped state (at 0 V vs. Ag pseudoreference electrode) is highlighted by a *bold curve*. The *topmost spectrum* was acquired at +1.8 V. The *spectra underneath the bold curve* were measured at potentials, which varied by steps of 0.2 V from 0 to 1.8 V vs. Ag pseudoreference electrode. Spectra are offset for clarity, but the intensity scale is identical for all spectra

potential. We may reasonably assume that the amount of acetonitrile in the optical path is not perturbed by electrochemistry; that is, the only changing component of the electrolyte solution is NBu_4^+. Thus, the growth of peaks downward oriented indicates the decrease of the NBu_4^+ concentration in the nanotube electrode and vice versa.

From the plot in Fig. 4, we can conclude that the anodic charging (p-doping) depletes NBu_4^+ species as the counterions in the SWNT film, and they are now replaced by BF_4^- anions (cf. spectra at 1.8 and 0 V). The opposite tendency for cathodic charging (n-doping) is less obvious from our spectra, because the C–H stretch overtones are superimposed on the ΔE_{11}^{S}, and this band changes its intensity in the reverse direction. If we denote the carbon atom in SWNT as C_{SWNT} (existing at the off-cell potential in its neutral state) and the corresponding doping level per carbon

atom, x, then the following reactions describe the electrochemical processes in our system:

Cathodic charging (n-doping):

$$x\left(\mathrm{NBu}_4^+\right) + x(\mathrm{e}^-) + (C_{\mathrm{SWNT}}) \rightarrow (C_{\mathrm{SWNT}})^{x-}\left(\mathrm{NBu}_4^+\right)_x \tag{4a}$$

Anodic charging (p-doping):

$$x\left(\mathrm{BF}_4^-\right) + (C_{\mathrm{SWNT}}) \rightarrow (C_{\mathrm{SWNT}})^{x+}\left(\mathrm{BF}_4^-\right)_x + x(\mathrm{e}^-) \tag{4b}$$

Equations 4a and 4b assume that the only effect of electrochemical treatment is the double-layer charging with the concomitant change of counterions, balancing the charge in SWNT film. This simple charging feedback can be reasonably supposed to occur at most potentials applied in this study. Solely at the highest negative potentials (around −1.8 V vs. Ag), we should consider an additional process, viz. irreversible chemical breakdown of the $(C_{\mathrm{SWNT}})^{x-}\left(\mathrm{NBu}_4^+\right)_x$ species (cf. Eq. 4a). This reaction leads to products, like α-aminoalkyl radicals, which are detectable by electron paramagnetic resonance [16]. With respect to this study, the electrochemical and Vis–NIR data acquired at potentials down to −1.5 V vs. Ag are not markedly perturbed by this decomposition.

The doping level, x, is available from the electrochemical charge transferred, which is most easily measured by cyclic voltammetry. Voltammetric charge transfer between the open circuit potential, E_{OCP}, and certain vertex potential, E, causes the doping toward the level x:

$$x = \frac{M_C}{F}\int_{E_{\mathrm{OCP}}}^{E} C\,dE \tag{5}$$

For the typical value of $C \cong 40$ F/g [4, 5], and $\Delta U = 1$ V, Eq. 5 yields $x \cong 0.005$ e^-/C-atom. If we approximate that the specific double-layer capacitance is constant near the E_{OCP} and is equal to that of graphite, ($C_{\mathrm{gr}} \cong 3$ μFcm^{-2}) [17–19], then we get the "electrochemical" surface area, S_{el} of:

$$S_{\mathrm{el}} = \mathrm{C_{gr}/C} \cong 1330\ \mathrm{m^2/g} \tag{6}$$

which is close to the theoretical surface area of a SWNT, if we model it as a one-sided graphene sheet ($S_{\mathrm{theo}} = 1{,}315$ m^2/g) [20]. Unfortunately, this agreement is only casual: The experimental surface areas from Brunauer/Emmett/Teller isotherms are smaller by a factor of about 4, which can be attributed to the fact that only the outer surface of a SWNT bundle is involved in the N_2 adsorption [20, 21] (the actual experimental values vary in broad interval between approximately 200 and 900 m^2/g, but the values around 300 m^2/g are reported most frequently for SWNT bundles [20]). As the charge transfer near the E_{OCP} is similarly addressing the outer surface of the rope, the value quoted in Eq. 5 is dubious. A way out seems to be an assumption of larger specific charge of SWNT (≅10 μFcm^{-2}) as suggested by Smalley et al. [22].

The quantitative evaluation of the charge conditions at the nanotube would deserve a detailed discussion, and the spectrophotometric tracing of counterions (cf. our data in Fig. 4 for NBu_4^+) can provide a useful analytical tool for this study. The potential dependence of the cation band and the bleaching of the VHS should be considered, and the contribution of the Faradaic charge transfer and the double layer charging can be separated. This approach is the subject of further investigations [5]. In this paper, we have demonstrated that the optical in situ spectroelectrochemistry at free-standing nanotube electrodes is a prerequisite for detailed studies of the charge transfer at carbon nanostructures.

Acknowledgments This work was supported by the Czech Ministry of Education Youth and Sports (contract No. LC-510) and by the IFW Dresden.

Reference

1. Rao AM, Eklund PC, Bandow S, Thess A, Smalley RE (1997) Nature 388:257
2. Sumanasekera GU, Allen JL, Fang SL, Loper AL, Rao AM, Eklund PC (1999) J Phys Chem B 103:4292
3. Kavan L, Rapta P, Dunsch L (2000) Chem Phys Lett 328:363
4. Kavan L, Rapta P, Dunsch L, Bronikowski MJ, Willis P, Smalley RE (2001) J Phys Chem B 105:10764
5. Kavan L, Dunsch L (2007) Chemphyschem 8:974
6. Kazaoui S, Minami N, Jacquemin R, Kataura H, Achiba Y (1999) Phys Rev B 60:13339
7. Petit P, Mathis C, Journet C, Bernier P (1999) Chem Phys Lett 305:370
8. Jacquemin R, Kazaoui S, Yu D, Hassanien A, Minami N, Kataura H, Achiba Y (2000) Synth Metals 115:283
9. Bendiab N, Anglaret E, Bantignies JL, Zahab A, Sauvajol JL, Petit P, Mathis C (2001) Phys Rev B 64:245424
10. Liu X, Pichler T, Knupfer M, Fink J, Kataura H (2004) Phys Rev B 69:0754171
11. Kavan L, Dunsch L (2003) Chemphyschem 4:944
12. Kazaoui S, Minami N, Kataura H, Achiba Y (2001) Synth Metals 121:1201
13. Kazaoui S, Minami N, Matsuda N, Kataura H, Achiba Y (2001) Appl Phys Lett 78:3433
14. Wu Z, Chen Z, Du X, Logan JM, Sippel J, Nikolou M, Kamaras K, Reynolds JR, Tanner DB, Hebard AF, Rinzler AG (2004) Science 305:1273
15. Arnold MS, Green AA, Hulvat JF, Stupp SI, Hersam MC (2006) Nature Nanotech 1:60
16. Tarabek J, Kavan L, Kalbac M, Rapta P, Zukalova M, Dunsch L (2006) Carbon 44:2147
17. Gerischer H (1987) J Phys Chem 91:1930
18. Gerischer H (1985) J Phys Chem 89:4251
19. Randin JP, Yeager E (1971) J Electrochem Soc 118:711
20. Peigney A, Laurent C, Flahaut E, Bacsa RR, Rousset A (2001) Carbon 39:507
21. Stoll M, Rafailov PM, Frenzel W, Thomsen C (2003) Chem Phys Lett 375:625
22. Claye AS, Fischer JE, Huffman CB, Rinzler AG, Smalley RE (2000) J Electrochem Soc 147:2845